





**FULL PAPER**

# Synthesis and mode of action studies of novel {2-(3-R-1H-1,2,4-triazol-5-yl)phenyl}amines to combat pathogenic fungi

Lyudmyla Antypenko<sup>1</sup>  | Zhanar Sadykova<sup>1</sup>  | Kostiantyn Shabelnyk<sup>2</sup>  |  
 Fatuma Meyer<sup>1</sup> | Sergiy Kovalenko<sup>2</sup>  | Vera Meyer<sup>3</sup> | Leif-Alexander Garbe<sup>1</sup> |  
 Karl Steffens<sup>1</sup>

<sup>1</sup>Department of Food and Bioproduct Technology, Neubrandenburg University, Neubrandenburg, Germany

<sup>2</sup>Departments of Pharmaceutical Chemistry, Organic and Bioorganic Chemistry, Zaporizhzhya State Medical University, Zaporizhzhya, Ukraine

<sup>3</sup>Department of Applied and Molecular Microbiology, Institute of Biotechnology, Technische Universität Berlin, Berlin, Germany

**Correspondence**

Dr. Lyudmyla Antypenko, Department of Food and Bioproduct Technology, Neubrandenburg University, Brodaer Street 2, 17033 Neubrandenburg, Germany.  
 Email: antypenkol@gmail.com

**Funding information**

Bundesministerium für Bildung und Forschung, Grant/Award Number: FKZ 03FH025IX4

**Abstract**

Due to their high specificity and efficacy, triazoles have become versatile antifungals to treat fungal infections in human healthcare and to control phytopathogenic fungi in agriculture. However, azole resistance is an emerging problem affecting human health as well as food security. Here we describe the synthesis of 10 novel {2-(3-R-1H-1,2,4-triazol-5-yl)phenyl}amines. Their structure was ascertained by liquid chromatography–mass spectrometry, <sup>1</sup>H and <sup>13</sup>C NMR, and elemental analysis data. Applying an in vitro growth assay, these triazoles show moderate to significant antifungal activity against the opportunistic pathogen *Aspergillus niger*, 12 fungi (*Fusarium oxysporum*, *Fusarium fujikuroi*, *Colletotrichum higginsianum*, *Gaeumannomyces graminis*, *Colletotrichum coccodes*, *Claviceps purpurea*, *Alternaria alternata*, *Mucor indicus*, *Fusarium graminearum*, *Verticillium lecanii*, *Botrytis cinerea*, *Penicillium digitatum*) and three oomycetes (*Phytophthora infestans* GL-1, *P. infestans* 4/91; R+ and 4/91; R-) in the concentration range from 1 to 50 µg/ml (0.003–2.1 µM). Frontier molecular orbital energies were determined to predict their genotoxic potential. Molecular docking calculations taking into account six common fungal enzymes point to 14α-demethylase (CYP51) and N-myristoyltransferase as the most probable fungal targets. With respect to effectiveness, structure–activity calculations revealed the strong enhancing impact of adamantyl residues. The shown nonmutagenicity in the *Salmonella* reverse-mutagenicity assay and no violations of drug-likeness parameters suggest the good bioavailability and attractive ecotoxicological profile of the studied triazoles.

**KEYWORDS**

{2-(3-R-1H-1,2,4-triazol-5-yl)phenyl}amines, Ames test, antifungal activity, drug-like descriptors, molecular docking, structure–activity relationship

**Abbreviations:** <sup>1</sup>H NMR, proton nuclear magnetic resonance; CYP51, P-450-dependent 14α-sterol demethylase; DMSO, dimethylsulfoxide; IP, ionization potential; LC–MS, liquid chromatography–mass spectrometry; LOMO, lowest-occupied molecular orbital; MFC, minimum fungicidal concentration; MIC, minimum inhibition concentration; MM+, molecular mechanics; MNDO, modified neglect of the diatomic overlap; MW, molecular weight; NMT, N-myristoyltransferase; PDA, potato dextrose agar; SAR, structure–activity relationship; Topo II, topoisomerase II; TPSA, molecular topological polar surface areas.

**1 | INTRODUCTION**

The control of phytopathogenic fungi is of paramount importance to avoid serious losses in agriculture and to protect food security and consumer safety for a growing world population. Until the 1940s, mainly inorganic antifungal substances were used. Since then, new

chemicals have been developed, which exhibited higher selectivity and less toxicity towards the environment and food consumers. In 2014, the volume of the global fungicide market was estimated to be about €10 billion.<sup>[1]</sup> Given that fungi are eukaryotic systems, it is not straightforward to find substances with sufficient discriminatory potential to act against the intended targets with low concomitant toxicity towards organisms requiring protection. Modern antifungals mainly act as inhibitors of ergosterol biosynthesis, membrane disruptors or interfere with biosynthesis of the cell wall, sphingolipids, nucleic acids, proteins, or microtubules. Most of them confer only fungistatic effects.<sup>[2]</sup>

Among ergosterol inhibitors, 1,2,4-triazoles have attained great importance in human healthcare<sup>[3]</sup> and are the most commonly used type of fungicides in agriculture with a market share of approximately 20%.<sup>[4]</sup> This success is based on the extraordinary activity of this class of antifungals. Spectroscopic analysis on purified *Candida albicans* P-450-dependent 14 $\alpha$ -sterol demethylase (CYP51) revealed, that triazoles interact with the sixth coordination position of the central iron of the P-450 heme active center.<sup>[5]</sup> The three-dimensional conformation of a full-length CYP51 14 $\alpha$ -lanosterol demethylase from *Saccharomyces cerevisiae* was elucidated by crystallization. The enzyme is anchored in the membrane of the endoplasmic reticulum with an N-terminal transmembrane  $\alpha$ -helix. CocrySTALLIZATION with sterol substrates confirmed earlier findings of the involvement of the heme group in the active center and amino acid residues in the near environment for catalytic function.<sup>[6]</sup>

The emergence of eucaryotic microorganisms including fungi with reduced susceptibility or resistance to drugs is a common phenomenon also observed with azoles.<sup>[7]</sup> Disturbingly, in clinical settings, triazole resistant pathogenic fungus *Aspergillus fumigatus* carrying alterations in gene CYP51A could be isolated from infected patients, who never before were treated with therapeutic azole drugs. This implies the fungus likely encountered resistance from the environment.<sup>[8,9]</sup> Physiological and genetic studies revealed that overexpression of drug efflux pumps or CYP51, modification of the ergosterol biosynthetic pathway, or mutations within the CYP51 gene are the main strategies for fungi to become resistant towards triazoles.<sup>[4]</sup> For instance, the replacement of a conserved tyrosine (Y140F/H) in the active site of CYP51 could be identified to confer resistance against short-chain azoles to a mutated *S. cerevisiae* strain.<sup>[10]</sup> In this context, the development of new substances is a necessity to secure the availability of active antifungals for agriculture and human healthcare in the future.<sup>[11]</sup>

In vitro experiments revealed that *N*-[2-hydroxy-3,3-dimethyl-2-[(1*H*-1,2,4-triazol-1-yl)methyl]butyl]benzamide derivatives (Figure 1a) bearing a triazole ring with a benzamide moiety displayed high antifungal activity against *Alternaria alternata* at 50  $\mu$ g/ml.<sup>[12]</sup>

Basarab et al.<sup>[13]</sup> reported that for most of the 1-amino-1,2,4-triazole (Figure 1b) fungicides, the basic structural requirement for activity against *Venturia inaequalis*, *Cercosporidium personatum*, *Pseudocercospora herpotrichoides*, *Erysiphe graminis*, and *Puccinia recondita* was a two-atom bridge connecting the azole nucleus to a hydrophobic group, typically an aromatic ring. However, still no

single compound had a clear advantage over standard fungicide flusilazole when considering the spectrum of activity. Applying a structure-activity relationship (SAR) analysis of aryl or hetaryl substituents for *N*-(4-(3-(2,4-dichlorophenyl)-3-oxo-2-(1*H*-1,2,4-triazol-1-yl)prop-1-en-1-yl)aryl)benzamides (Figure 1c), Tang et al.<sup>[14]</sup> supposed an antifungal activity against *Gibberella azea*, when a 2-hydroxy group or 4-chloro substituent was introduced into the phenyl ring. *Fusarium oxysporum*, *Cytospora mandshurica*, and *Pellicularia sasakii* were inhibited when the phenyl residue was replaced by a furan-2-yl moiety. The 3-(adamantan-1-yl)-4-ethyl-5-(*R*-methylthio)-4*H*-1,2,4-triazoles **D1** and **D2**<sup>[15]</sup> had a in vitro stronger fungistatic and fungicidal activity against *Candida albicans*, than the reference agent, trimethoprim. Their minimum inhibition concentrations (MIC) were 31.25 and 7.8  $\mu$ g/ml, and the minimum fungicidal concentrations (MFC) were 62.5 and 15.6  $\mu$ g/ml, respectively. Among the hiourea substituted series, 2-(2-((5-(adamantane-1-yl)-4-phenyl-1,2,4-triazole-3-yl)thio)acetyl)-*N*-ethyl-hydrazinecarbothioamide (Figure 1e) appeared the most active in relation to all microbial test-strains (*Staphylococcus aureus*, *Escherichia coli*, *Pseudomonas aeruginosa*, *C. albicans*)<sup>[16]</sup> with an MIC and MFC of 31.25  $\mu$ g/ml against *C. albicans*. The antifungal activities of the myrtenal bearing 1,2,4-triazoles **F** were evaluated against *Fusarium wilt* on cucumber (*F. oxysporum*), apple root spot (*Physalospora piricola*), tomato early blight (*Alternaria solani*), speckle on peanut (*Cercospora arachidicola*), and wheat scab (*Gibberella zeae*) at 50  $\mu$ g/ml.<sup>[17]</sup> The *i*-propyl **F1**, *O*-nitrobenzyl **F2** and ethyl **F3** thioethers exhibited excellent antifungal activity against *P. piricola* with inhibition rates of 98.2%, 96.4%, and 90.7%, respectively, showing better or comparable antifungal activity than that of the commercial fungicide azoxystrobin with a 96.0% inhibition rate. Molecular docking studies confirmed the experimental results showing that 2-aryl-4-[(6-substituted-2-(aryloxy)-quinolin-3-yl)-methyl]-3*H*-1,2,4-triazol-3-ones (Figure 1g) were active against *A. fumigatus* and *C. albicans* (MIC 0.2–1.5  $\mu$ g/ml).<sup>[18]</sup> Analogs containing methoxy and chloro substituents (**J1–3**) exhibited the strongest activity. And *N*-myristoyltransferase transferase (NMT) and dihydrofolate reductase were identified as the most probable target enzymes.

Moreover, it was found that molecular orbital calculations such as semiempirical methods (MM+ and MNDO) allowed deriving a theoretical estimation of the reactivity, and thereby the potential toxicity of novel substances. Namely, linear dependences are described between the LUMO energy of the different nitroaromatic compounds,<sup>[19]</sup> methylnitro- and aminocarbazoles,<sup>[20]</sup> nitrobenzanthrones,<sup>[21]</sup> and potential gene toxicity as can be detected by bioassays as the *Salmonella* mutagenicity test.<sup>[22]</sup>

Encouraged by these observations, we explored the antifungal potential of our {2-(3-*R*-1*H*-1,2,4-triazol-5-yl)phenyl}amines with special focus on phytopathogenic fungi. Here, we present the synthesis, structural elucidation, and in vitro antifungal activities of 10 novel {2-(3-*R*-1*H*-1,2,4-triazol-5-yl)phenyl}amines, bearing cycloalkyl, hetaryl, and halogen residues. Reactivity and thereby the potential toxicity of the substances is estimated by semiempirical methods (MM+ and MNDO), namely, frontier molecular orbital

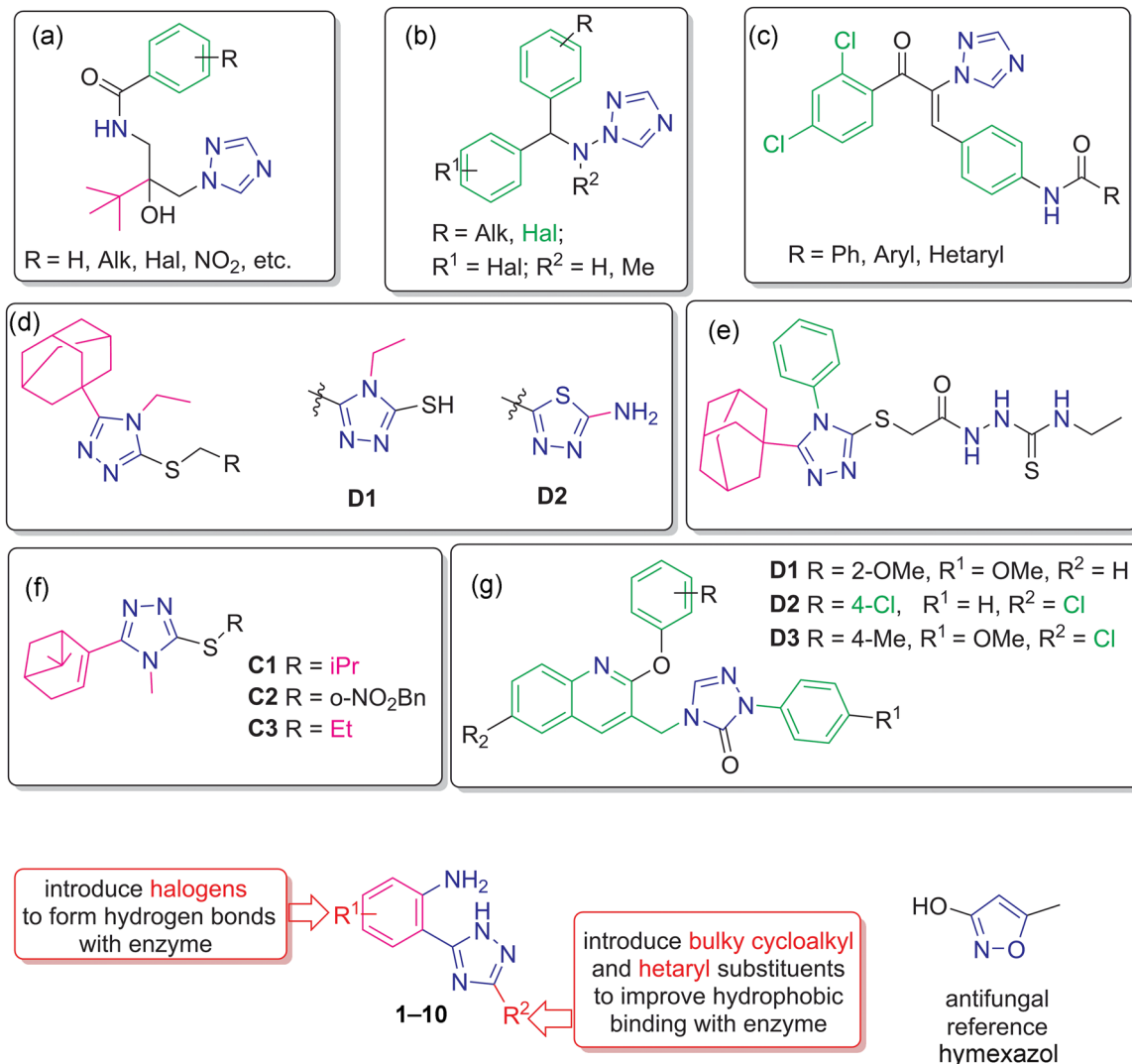


**FIGURE 1** Reported fungicides containing a triazole ring with types of functional fragments, which were purposefully introduced into novel synthesized substances (a–j, 1–10), and the antifungal reference hymexazol

calculations. Additionally, triazoles' affinities are calculated to the six common fungal enzymatic targets. The findings are discussed with respect to mutagenicity potential, which is determined with the reverse *Salmonella* mutagenicity assay.

## 2 | RESULTS AND DISCUSSION

### 2.1 | Synthesis

The antifungal SAR reported by Zhang et al.,<sup>[12]</sup> Basarab et al.,<sup>[13]</sup> and Tang et al.<sup>[14]</sup> led us to synthesize and analyze novel {2-(3-*R*)-1*H*-1,2,4-triazol-5-yl}phenylamines 1–10 with different cycloalkyl and hetaryl substituents (Figure 2, Supporting Information).

Quinazolin-4-ones **b** were obtained by heating the corresponding derivatives of anthranilic acid **a** with formamide (Nimetovsky reaction).<sup>[23,24]</sup>

Substances **b** were thionated to **c** by  $\text{P}_2\text{S}_5$  refluxing in xyol.<sup>[25]</sup> Then 4-hydrozinoquinazolines **e** were obtained by hydrazinolysis of **c**

in isopropanol media.<sup>[26]</sup> The latter could be synthesized alternatively through formation of 4-chloroquinazolines **d** by treatment of quinazolin-4-ones **b** with  $\text{PCl}_5$  and  $\text{POCl}_3$ , followed also by hydrazinolysis.<sup>[26]</sup> Synthesis of (3*H*-quinazolin-4-ylidene)hydrazides of cycloalkyl-(hetaryl)carboxylic acids **f** as useful precursors to obtain the corresponding tricyclic derivatives **g** was carried out in two ways: reaction of substances **d** with the appropriate carboxylic acid hydrazides or acylation of substances **e** by imidazolides of carboxylic acids.<sup>[27–29]</sup> The 2-cycloalkyl-(hetaryl)-[1,2,4]triazolo[1,5-*c*]quinazolines **g** were synthesized by dehydration of substances **f** in a medium of glacial acetic acid with usage of a Dean-Stark receiver.<sup>[28–30]</sup> As shown by Kovalenko et al.,<sup>[31]</sup> derivatives **g** were electron-deficient systems evidenced by the deshielded H-5 singlet found at 9.85–9.25 ppm in the proton nuclear magnetic resonance ( $^1\text{H}$  NMR) spectra. The high electrophilic properties of C-5 promoted the nucleophilic addition reaction followed by the degradation of the pyrimidine ring<sup>[32–34]</sup> to form the appropriate 1–10 in water under acid catalysis.

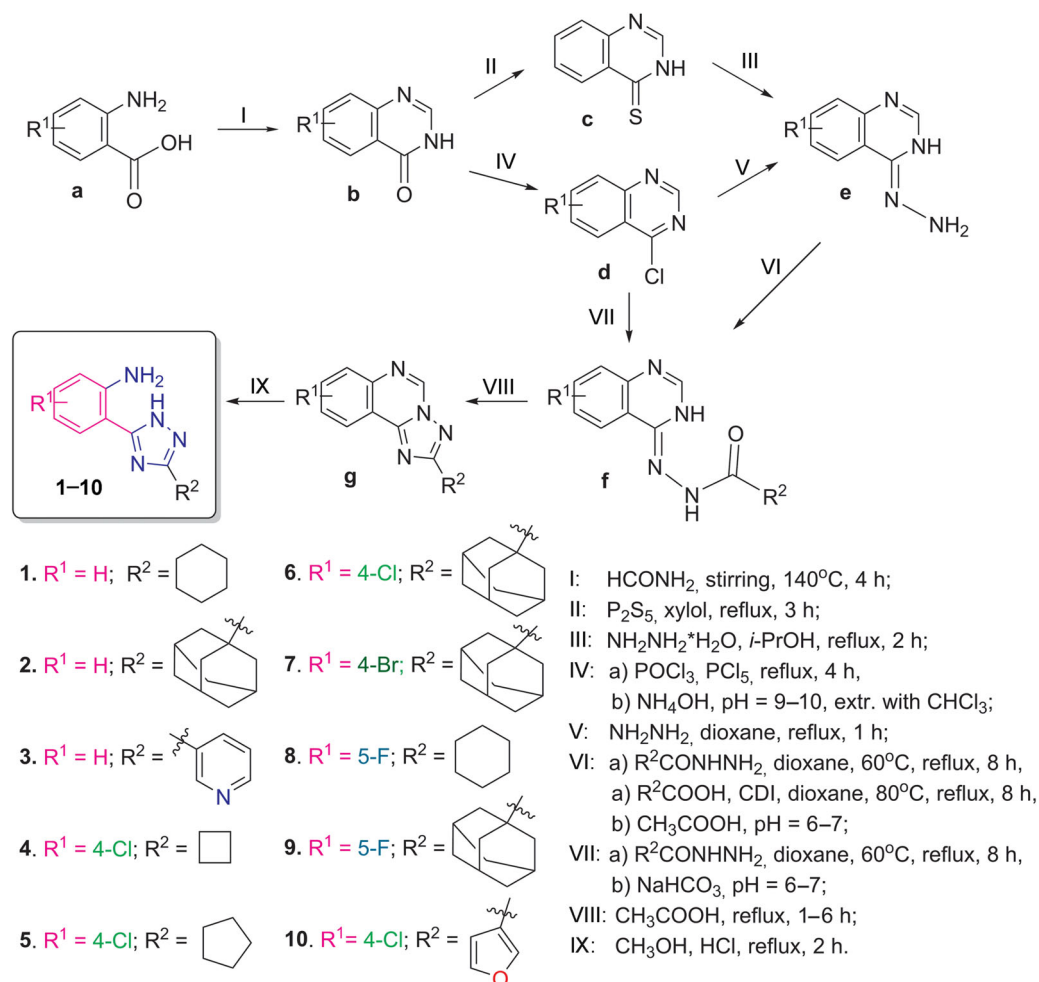


**FIGURE 2** The synthetic route of {2-(3-R)-1H-1,2,4-triazol-5-yl]phenyl]amines (1–10)

According to the spectral data, the products of the above mentioned reaction were identified as the corresponding {2-(3-R-1H-1,2,4-triazole-5-yl)phenyl]amines (1–10). The liquid chromatography–mass spectrometry (LC–MS) spectra were characterized by intensive peaks of quasimolecular ions  $[M+1]^+$  indicating a high purity of products. The elemental analysis data confirmed the empirical formulas of synthesized substances.

In  $^1H$  NMR spectra, the broadened proton singlet of  $NH_2$  group was registered at 6.60–6.17 ppm and the doubled or broadened signal of the triazole ring's proton turned up in the low field at 14.54–13.23 ppm. The signals of aminophenyl fragments of substances 1–3 appeared as unresolved doublets at 7.98/7.54 (H-3) and 6.45/6.58 (H-6) ppm, and triplets at 6.68–6.70 (H-4) and 6.99–6.11 (H-5) ppm. The doubling or broadening of the signals was associated with tautomeric transformations of the synthesized compounds.<sup>[32,33]</sup> Moreover,  $^1H$  NMR spectra of 1–10 were characterized by signals of all other substituents with the common multiplicity and chemical shifts.

In  $^{13}C$  NMR spectra, it was found that signals caused by  $C_3$  and  $C_5$  atoms of triazole cycle were observed as broad singlets at 164.6–157.1 and 163.9–148.7 ppm for 1–10. Doubling of  $C_3$  and  $C_5$  signals of the aniline fragment was observed in the spectrum for

compounds 2, 4, 5, and 10 due to their azole–azole tautomerism. Significant paramagnetic shift of  $C_1$  atom (149.0–145.8 ppm) was caused by the primary amino group and indicated the hydrolytic cleavage of the pyrimidine cycle. The other carbon atoms of the aryl fragment and the substituents in position 2 had chemical shifts that corresponded to the proposed structures.

## 2.2 | Molecular docking studies

We modeled the potential interaction of the triazoles with sterol  $14\alpha$ -demethylase (CYP51) by flexible molecular docking<sup>[35]</sup> to predict the antifungal mode of action in silico. The cytochrome P-450-type enzyme is involved in the biosynthesis of ergosterol, an essential plasma membrane constituent of lower eukaryotes. Namely, azoles are known to block the de novo biosynthesis of ergosterol,<sup>[3,5]</sup> and thereby not only deplete its source for the buildup of membranes, but also prevent the formation of physiologically important intracellular sterols, which are required for cell-cycle regulation, multiplication,<sup>[36]</sup> and cell transformation.<sup>[37]</sup> The crystal structure of CYP51 from *C. albicans* in complex with the tetrazole-based antifungal drug candidate VT1161 was downloaded from the Protein Data Bank (PDB; ID: 5TZ1).<sup>[35]</sup> As reference, hymexazol

(3-hydroxy-5-methylisoxazole; Figure 1) was chosen owing to its structural resemblance and comparable activity.<sup>[14]</sup> The calculated affinity score with the minimum energy indicate a high structural ligand–protein complex matching for all substances (Table 1).

The affinity of all compounds towards CYP 51 exceeded that of hymexazol. The strongest affinity was calculated for adamantyl substituted triazoles: 2-(3-(adamantan-1-yl)-1H-1,2,4-triazol-5-yl)-5-fluoroaniline (**9**), 4-bromoaniline (**7**), and 4-chloroaniline (**6**). In addition to hydrophobic interactions of adamantyl residues, substances **6**, **7**, and **9** formed several hydrogen bonds with serine 507, 378, and methionine 508, involving triazole NH-groups and halogen substituents (Figure 3, Supporting Information). Apart from these observations, Hargrove et al.<sup>[36]</sup> emphasized that *C. albicans* CYP51 was more strongly inhibited by clinical azoles with elongated side chains.

Interestingly, the interaction of triazoles with the P-450 demethylase heme group, as described by Hitchcock et al.,<sup>[5]</sup> could only be modeled for hymexazol and substances without the adamantyl fragment (**1**, **3–5**, **8**, **10**), but not for substances **2**, **6**, **7**, and **9**, which show the highest scoring functions (Supporting Information). However, this is not the only enzyme that may be affected by the studied compounds. So, it was decided to conduct in silico molecular docking to further five common antifungal targets.<sup>[35]</sup> The calculations revealed that the tested triazoles indeed interact with all of them and even with a higher probability than the reference agent, hymexazol (Table 1). The triazoles in this study show a strong affinity score to NMT only after CYP51, like the previously reported by Somagond et al.<sup>[18]</sup> substituted quinolines containing a 1,2,4-triazole moiety. Notably, affinity prediction to enzymes taken from *Candida albicans* (CYP51, NMT, and secreted aspartic proteinase) has shown the best scores. The lowest affinity (mean for **1–10**: –6.7 kcal/mol) was determined for L-glutamine:D-fructose-6-phosphate aminotransferase (GlcN-6-P). Averaged over all calculated targets, substances **9**, **2**, **6**, and **7** showed the highest level of affinity (–8.9 to –8.4 kcal/mol).

The polarity of the substances gives an indication of their potential to penetrate the cell membrane and to enter the relative

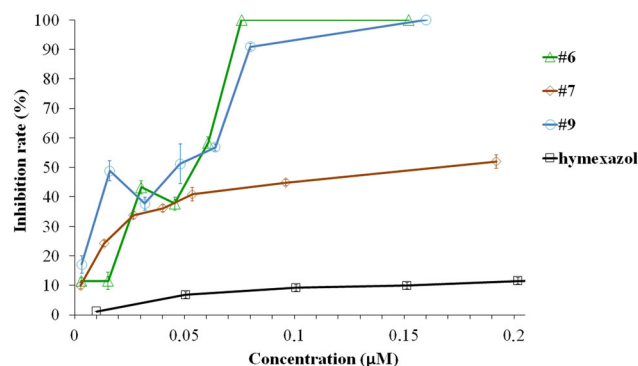


**FIGURE 3** Growth inhibition of *Colletotrichum higginsianum* by substances **6**, **7**, and **9** and antifungal reference hymexazol (hym). Error bars indicate standard deviation of at least three experiments

**TABLE 2** The calculated distribution coefficient (log D) at pH 2–9 in order of lipophilicity decrease

Substance	Log D at pH			
	2	4	7.4	9
<b>7</b>	3.88	4.72	4.70	3.63
<b>6</b>	3.87	4.52	4.49	3.40
<b>9</b>	3.66	4.11	4.09	3.09
<b>2</b>	2.77	3.91	3.94	2.91
<b>8</b>	3.08	3.54	3.53	2.75
<b>5</b>	2.90	3.53	3.52	2.61
<b>1</b>	2.18	3.34	3.38	2.54
<b>10</b>	2.51	3.00	3.00	2.45
<b>4</b>	2.50	3.11	3.10	2.19
<b>3</b>	–0.02	1.81	1.97	0.78
Hymexazol	0.83	0.81	–0.97	–1.3

hydrophobic binding site of CYP51. Therefore, log D was calculated assuming an average cytoplasmic pH at 7.4 for fungal cells (for instance, *Aspergillus niger*<sup>[38]</sup>; Table 2). At this pH level, except for

**TABLE 1** Calculated affinities of tested triazoles and reference hymexazol (hym) to common antifungal enzymatic targets (from *Candida albicans* (CYP51, NMT, SAP2), *Escherichia coli* (MurD, GlcN-6-P), and *Sacchomyces cerevisiae* (Topo II))

Target enzyme	PDB code	Affinity (kcal/mol)											
		hym	<b>9</b>	<b>2</b>	<b>6</b>	<b>7</b>	<b>8</b>	<b>1</b>	<b>3</b>	<b>5</b>	<b>10</b>	<b>4</b>	Mean
14α-Demethylase (CYP51)	5TZ1	–4.3	<b>–11.1</b>	<b>–10.5</b>	<b>–11.0</b>	<b>–11.0</b>	–9.8	–9.6	–9.1	–9.2	–8.4	–8.5	–9.8
N-Myristoyltransferase (NMT)	1IYL	–4.9	<b>–9.5</b>	–9.2	<b>–9.6</b>	<b>–9.7</b>	–8.9	–8.9	–8.4	–8.7	–8.0	–8.1	–8.9
Secreted aspartic proteinase (SAP2)	1EAG	–3.9	<b>–8.6</b>	–8.4	<b>–8.5</b>	<b>–8.7</b>	–8.0	–8.1	–7.5	–8.1	–7.6	–7.7	–8.1
Topoisomerase II (Topo II)	1Q1D	–4.7	<b>–8.2</b>	<b>–7.8</b>	–7.2	–7.0	<b>–7.6</b>	–6.8	–7.5	–7.2	–7.4	–6.6	–7.3
UDP-N-acetyl-muramoyl-L-alanine:D-glutamate ligase (MurD)	1UAG	–4.4	<b>–7.9</b>	–7.6	<b>–7.8</b>	<b>–7.7</b>	–7.1	–6.9	<b>–7.7</b>	–6.8	–7.0	–6.6	–7.3
L-Glutamine:D-fructose-6-phosphate aminotransferase (GlcN-6-P)	1XFF	–4.8	<b>–7.8</b>	<b>–7.2</b>	–6.3	–6.3	<b>–6.9</b>	–6.7	–6.5	–6.4	–6.5	–6.6	–6.7
Mean		–4.5	<b>–8.9</b>	–8.5	–8.4	–8.4	–8.1	–7.8	–7.8	–7.7	–7.5	–7.4	–

Note: In the order from highest to lowest average data. Bold values designate substances with the three highest affinities to the mentioned enzyme.



substance **3**, all triazoles appeared to be more lipophilic than the reference compound hymexazol.

Danby et al.<sup>[39]</sup> investigated the influence of pH on the in vitro antifungal activity level of drugs and demonstrated that under conditions of lowered pH (4–5), *Candida glabrata* isolates remained susceptible to caspofungin and flucytosine. At the same time, there was a dramatic increase of sensitivity to amphotericin B, fluconazole, voriconazole, posaconazole, itraconazole, ketoconazole, and other triazole agents. Therefore, log D was also calculated for the newly synthesized substances at various pH (Table 2).

Basically, log D remained unchanged at pH 7.4 and 4.0. Only at pH 2 and 9 was the ionization state of substances affected with a concomitant reduced lipophilicity by protonation and deprotonation, respectively. In this context, it may also be considered that after the addition of antifungal agents, the intracellular pH of fungi could be changed. Ullah et al.<sup>[40]</sup> monitored the intracellular pH of *C. glabrata* under the influence of antifungals caspofungin or amphotericin B with the pH-sensitive probe GFP ratiometric pHluorin: in media at pH 4, the drugs caused an acidification of the cytoplasm, whereas in media at pH 7.4, a slight alkalization was observed. These broad physiological reactions may interfere with normal cell metabolism and fungal growth as with the susceptibility towards antifungal drugs such as triazole inhibitors of CYP51 demethylase.

## 2.3 | Fungal proliferation and antifungal activity

The in silico modeling approach and log D data strongly suggest that the newly synthesized triazoles should penetrate the cell membrane and interact with the CYP51 active site, thereby provoking an antifungal effect at a similar or higher level as compared to the reference

compound hymexazol 50 µg/ml (0.5 µM). As shown in Table 3, a significant antifungal activity could be observed for all tested substances in a concentration of 50 µg/ml (0.13–0.21 µM) by mycelial growth rate assay<sup>[14]</sup> against other opportunistic pathogen *A. niger*, 12 fungal (*F. oxysporum*, *Fusarium fujikuroi*, *Colletotrichum higginsianum*, *Gaeumannomyces graminis*, *C. coccodes*, *Claviceps purpurea*, *A. alternata*, *Mucor indicus*, *Fusarium graminearum*, *Verticillium lecanii*, *Botrytis cinerea*, *Penicillium digitatum*) and three oomycete (*Phytophthora infestans* GL-1, *P. infestans* 4/91; R+ and 4/91; R-) strains.

The effects were very different depending on the type of triazole and tested organism. The synthesized substances inhibited majority of the fungi, among which **10**, **6**, **9**, **2**, and **8** had the best results. *F. fujikuroi* was the most sensitive strain (89.7% of inhibition), whereas at the other end, *A. niger* showed the highest level of resistance (13.9% of inhibition). Interestingly, with respect to therapeutic triazoles, acquired resistance of *A. fumigatus* is an often described phenomenon, which may be based on similar mode(s) of action.<sup>[41]</sup> In addition, generally, the tested *Phytophthora* strains (24.2–34.2% of inhibition) were difficult to inhibit by triazoles (including reference substance hymexazol), which may reflect their distinct physiology as belonging to the oomycete group. Interestingly, hymexazol and substance **3** were completely ineffective towards *M. indicus*. And, at the same time substances **5** and **10** at least brought about 70% of inhibition.

The growth of strains *G. graminis*, *C. higginsianum*, *C. coccodes*, *C. purpurea*, and *A. alternata* was inhibited practically at 60% by all substances. But, when calculating the average activity of the strongest substances (**10**, **6**, **9**, **2**, and **8**), the above mentioned fungi were sensitive at almost 70–80%. Moreover, in comparison to *N*-(4-(3-(2,4-dichlorophenyl)-3-oxo-2-(1*H*-1,2,4-triazol-1-yl)prop-1-en-1-yl)

**TABLE 3** Growth inhibition rate of tested triazoles **1–10** and hymexazol at 50 µg/ml

Substance	µM	Growth inhibition rate (%)																Mean
		FF	GG	CH	CC	CP	AA	FO	MI	FG	VL	BC	PD	PI GL-1	PI p-3	PI p-4	AN	
hym.	0.50	<b>85.7</b>	28.0	32.9	56.1	50.9	<b>95.8</b>	41.6	0.0	34.4	<b>100.0</b>	<b>95.6</b>	0.0	51.5	33.2	30.4	17.1	47.1
<b>10</b>	0.19	<b>95.2</b>	<b>98.8</b>	<b>70.2</b>	<b>70.3</b>	<b>100.0</b>	<b>87.8</b>	<b>61.4</b>	<b>69.4</b>	59.8	<b>100.0</b>	47.8	18.9	49.5	32.3	18.7	16.3	<b>62.3</b>
<b>6</b>	0.15	<b>81.0</b>	<b>100.0</b>	<b>100.0</b>	<b>72.5</b>	57.1	<b>63.4</b>	59.5	52.5	59.1	33.5	37.7	41.8	56.8	16.7	35.3	41.2	56.8
<b>9</b>	0.16	<b>90.1</b>	<b>100.0</b>	<b>100.0</b>	<b>70.1</b>	46.7	<b>63.4</b>	34.5	53.9	<b>61.2</b>	31.2	57.2	41.1	29.0	38.1	13.8	–2.4	51.7
<b>2</b>	0.17	<b>93.8</b>	52.9	48.8	<b>72.5</b>	49.2	57.1	<b>62.6</b>	72.1	46.0	36.4	64.6	37.7	45.5	35.3	18.7	19.4	50.8
<b>8</b>	0.19	<b>88.6</b>	52.0	47.2	57.4	<b>94.2</b>	<b>69.0</b>	<b>63.3</b>	59.3	49.5	43.9	35.7	33.0	41.6	36.7	34.6	–4.8	50.1
<b>5</b>	0.19	<b>64.5</b>	34.9	<b>60.7</b>	57.4	<b>100.0</b>	57.1	58.8	71.4	51.5	12.6	29.0	31.6	44.2	22.9	28.9	42.0	48.0
<b>4</b>	0.20	<b>85.7</b>	35.5	49.6	52.3	56.1	58.1	34.5	42.4	45.4	33.5	18.9	27.6	41.6	27.0	18.6	–7.1	38.7
<b>7</b>	0.13	<b>100.0</b>	<b>86.3</b>	<b>68.7</b>	<b>65.8</b>	26.4	41.8	28.8	18.9	21.3	23.7	9.8	18.9	23.8	15.9	11.3	–0.1	35.1
<b>1</b>	0.21	<b>100.0</b>	16.1	34.5	50.5	49.2	32.8	39.0	25.6	20.6	47.4	27.0	17.5	7.9	13.9	33.3	–2.4	32.1
<b>3</b>	0.21	<b>100.0</b>	28.7	18.7	21.9	3.3	25.7	25.6	0.0	6.9	39.9	25.6	8.1	2.0	14.1	28.4	–8.6	21.3
Mean (1–10)	–	<b>89.9</b>	<b>60.5</b>	59.8	59.1	58.2	55.6	46.8	46.5	42.1	40.2	35.3	27.6	34.2	25.3	24.2	9.35	–
Mean (2, 6, 8–10)	–	<b>89.7</b>	<b>80.7</b>	<b>73.2</b>	<b>68.6</b>	<b>69.4</b>	<b>68.1</b>	56.3	61.4	55.1	49.0	48.6	34.5	44.5	31.8	24.2	13.9	–

Note: Bold values indicate more than 60.0% of inhibition.

Abbreviations: AA, *Alternaria alternata*; AN, *Aspergillus niger*; BC, *Botrytis cinerea*; CC, *Colletotrichum coccodes*; CH, *Colletotrichum higginsianum*; CP, *Claviceps purpurea*; FF, *Fusarium fujikuroi*; FG, *Fusarium graminearum*; FO, *Fusarium oxysporum*; GG, *Gaeumannomyces graminis*; hym., hymexazol; MI, *Mucor indicus*; PD, *Penicillium digitatum*; PI GL-1, *Phytophthora infestans*; PI-3, *P. infestans* p-3; PI-4, *P. infestans* p-4; VL, *Verticillium lecanii*.

aryl)benzamides (Figure 1c) studied by Tang et al.<sup>[14]</sup> at 50 µg/ml, half of the {2-(3-R-1H-1,2,4-triazol-5-yl)phenyl}amines presented here were more active against *F. oxysporum* and practically all are stronger against *P. infestans*.

A moderate growth level (27–47%) was shown by *F. oxysporum*, *M. indicus*, *F. graminearum*, *V. lecanii*, *B. cinerea*, and *P. digitatum*.

A residual concentration of 1% DMSO (dimethylsulfoxide) in potato dextrose agar (PDA) test plates was necessary to ensure an even distribution of the lipophilic triazoles. Notably, this caused a stress phenotype on *A. niger*, which became evident by a black colorization of the mycel instead of yellow. Similar effects were not observed with the other strains.

In accordance with docking studies, **9**, **8**, **6**, and **2** were among the five most active substances. And, in summary the growth inhibition data reflect the result from in silico docking analysis and calculated lipophilicity. However, a notable exception is compound **10** combining the second lowest affinity with the best antifungal activity. Generally, the data reveal that chemicals may have quite different antifungal potentials. Nevertheless, in this context, docking studies are valuable tools to select most promising structures to develop highly active antifungals.

So, due to the revealed strong activity, it was decided to test substances **6**, **7**, and **9** along with the reference compound against one of the fungi, namely *C. higginsianum*, at lower concentrations to demonstrate the good antifungal potential of substances for further studies. In the concentration range of 0.0027–0.2 µM, all three compounds (**6**, **7**, and **9**) still had a higher antifungal activity than hymexazol at 0.01–0.2 µM (Figure 3).

Compound **9** showed decrease of antifungal activity, when the concentration was increased from 5 to 10 µg/ml (0.016–0.032 µM). This counter-intuitive characteristic, which to a lesser extent was also observed for substance **6** at 15 µg/ml (0.046 µM), may reflect a hormesis effect (toxicological concept characterized by low-dose stimulation and high-dose inhibition). Such phenomena have to be considered to adjust the dosage of antifungal agents to secure the most effective protection at the lowest necessary input. Substance **7** increased the level of inhibition in proportion to applied concentrations.

### 2.3.1 | Molecular docking visualization

Moreover, for the most active substance **10** (Table 4), a visual representation of the binding in the active sites of *N*-myristoyltransferase (1IYL) and 14- $\alpha$ -demethylase (5TZ1) is shown in Figure 4a,b, and these are calculated as targets of its strongest affinity (Table 1).

As listed in Table 4, substance **10** formed 13 bonds with *N*-myristoyltransferase, among which three are conventional hydrogen bonds due to connection to oxygen (with TYR 335 and LEU 450 and 451). In contrast, for 14- $\alpha$ -demethylase, only one conventional hydrogen bond was shown with TYR 123, among 12 possible ones.

**TABLE 4** List of calculated bonds between substance **10** and *N*-myristoyltransferase (1IYL) or 14- $\alpha$ -demethylase (5TZ1) active sites

Name	Å	Category	Type
(a) <i>N</i> -Myristoyltransferase (1IYL)			
:UNL1:H - B:TYR335:OH	2.05	Hydrogen bond	Conventional
:UNL1:H - B:LEU450:O	2.58	Hydrogen bond	Conventional
:UNL1:H - B:LEU451:OXT	2.33	Hydrogen bond	Conventional
:UNL1:C - B:LEU451:O	3.57	Hydrogen bond	Carbon
:UNL1:C - B:TYR119:OH	3.32	Hydrogen bond	Carbon
B:LEU451:OXT - :UNL1	3.32	Electrostatic	Pi-anion
:UNL1 - B:PHE117	4.37	Hydrophobic	Pi-pi stacked
B:TYR354 - :UNL1	4.82	Hydrophobic	Pi-pi T-shaped
:UNL1:CL - B:LEU394	5.25	Hydrophobic	Alkyl
B:TYR225 - :UNL1:CL	4.13	Hydrophobic	Pi-alkyl
B:TYR354 - :UNL1:CL	5.49	Hydrophobic	Pi-alkyl
:UNL1 - B:LEU394	4.74	Hydrophobic	Pi-alkyl
:UNL1 - B:LEU337	5.29	Hydrophobic	Pi-alkyl
(b) 14- $\alpha$ -Demethylase (5TZ1)			
:UNL1:H - A:TYR132:OH	2.71	Hydrogen bond	Conventional
A:TYR132:OH - :UNL1	3.59	Hydrogen bond	Pi-donor
A:HEM601 - :UNL1	3.97	Hydrophobic	Pi-pi stacked
:UNL1 - A:TYR118	4.03	Hydrophobic	Pi-pi stacked
:UNL1 - A:TYR118	4.95	Hydrophobic	Pi-pi T-shaped
:UNL1 - A:TYR132	5.36	Hydrophobic	Pi-pi T-shaped
A:HEM601:CMD - :UNL1:CL	3.43	Hydrophobic	Alkyl
:UNL1:CL - A:ILE131	3.39	Hydrophobic	Alkyl
A:HEM601 - :UNL1:CL	4.90	Hydrophobic	Pi-alkyl
:UNL1 - A:HEM601:CMD	4.31	Hydrophobic	Pi-alkyl
:UNL1 - A:LEU121	5.00	Hydrophobic	Pi-alkyl
:UNL1 - A:LEU376	5.28	Hydrophobic	Pi-alkyl

### 2.3.2 | Structure–activity relationship

It was found that change of the electron-withdrawing substituent (pyridine-3-yl) to electron-donating ones (cyclohexyl and adamantyl) (**3** < **1** < **2**), expansion of the cyclobutyl ring to adamantyl, introduction of the furan-3-yl substituent into the third position of the triazole ring (**4** < **5** < **6** < **10**), and fluorine introduction to the 2-phenyl fragment (**1** < **8**) led to an increase of the antifungal activity rate as well as a widened range of susceptible fungi (Figure 5).

It is notable that for fluorine containing substances **8** and **9**, there was practically no difference of antifungal activity, when the cyclohexyl residue was replaced by adamantyl, aiming at a higher fluorine impact on the activity rate. But, for **9** and **6** there was a difference for fluorosubstitution and chlorosubstitution, when bearing the adamantyl residue. Besides this, chloroderivative **6** had better activity than bromosubstituted **7**, and practically the same inhibition rate was observed for substance **2** bearing no halogen, showing the supremacy of adamantyl ring in possessing antifungal properties.

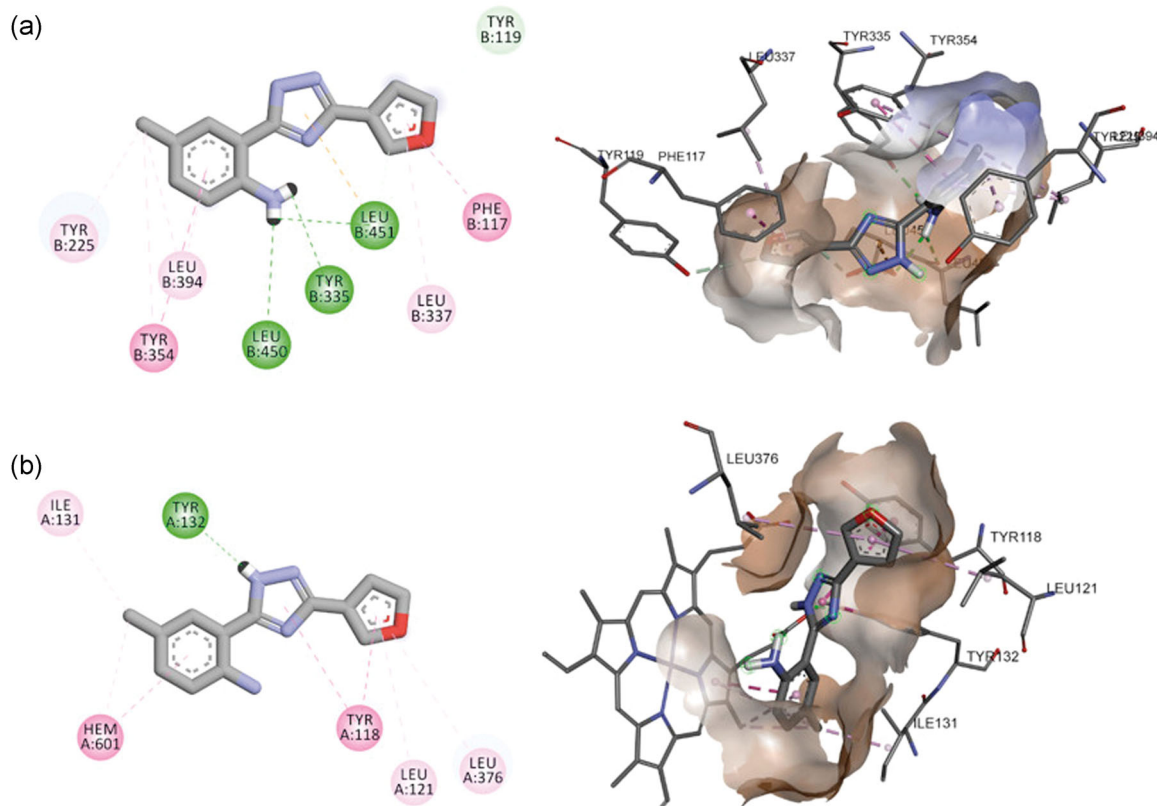


**FIGURE 4** Visual representation (2D and 3D) of the substance **10** showing bond formation and position in the active site of (a) N-myristoyltransferase (1IYL) and (b) 14- $\alpha$ -demethylase (5TZ1). Light blue: carbon hydrogen bond, green: classical conventional hydrogen bond, purple: hydrophobic  $\pi$ - $\pi$  stacked bond, pink: hydrophobic alkyl and  $\pi$ -alkyl bonds

And, also substances with no halogen (**1**) or with pyridin-3-yl (**3**) substituents exhibited the lowest growth inhibition effects. It is worth mentioning that **3** has the lowest lipophilicity according to calculated log D (Table 2).

And the findings on furan-3-yl **10**, which has strong activity, corresponds to the SAR analysis on furan-2-yl substituted compounds of Tang et al.<sup>[14]</sup>

## 2.4 | Safety evaluation of triazoles

### 2.4.1 | Frontier molecular orbitals calculations

Each novel substance needs a thorough safety evaluation, at least with respect to human health and environmental friendliness, before application in industrial processes, agriculture or medical care. Generally, it was found that lipophilic compounds with low-energy LUMOs were highly likely to be mutagenic, hence possibly carcinogenic. Hence, these parameters should be evaluated in the course of the development of drugs.<sup>[19–21]</sup> We investigated these characteristics for the novel triazoles by calculating important physical descriptors using density functional theory with the help of the calculated HOMO–LUMO (highest occupied molecular orbital–lowest unoccupied molecular orbital) energies<sup>[35]</sup> (Supporting Information) and testing the mutagenic potential with *Salmonella* reverse-mutagenicity in vitro assay (Ames test).

And according to the calculated descriptors the investigated substances are not highly reactive, hard electrophiles with  $\mu = -4.86 \pm 0.18$  eV,  $\eta = 4.32 \pm 0.14$  eV, and  $\omega = 2.73 \pm 0.16$  eV; the values are roughly at the level as those for reference hymexazol ( $\mu = -5.12$  eV,  $\eta = 5.00$  eV, and  $\omega = 2.62$  eV; Supporting Information). Due to the presence of additional heterocyclic rings in the molecular structure (pyrimidine or furan, respectively), substances **3** and **10** showed the lowest hardness with  $\eta = 4.09$  and  $4.04$  eV, correspondingly pointing to an elevated biochemical reactivity. Still, the electrophilicity index of substance **3** was lower than that of substance **10** with  $2.52$  against  $2.72$  eV, making the latter the most reactive among all synthesized substances besides **8** and **9** with an  $\omega = 2.93$  and  $2.91$  eV, respectively. Additionally, the substances were screened for pan-assay interference compounds<sup>[35]</sup> by means of a Badapple (bioactivity data associative promiscuity pattern learning engine) algorithm for identifying likely promiscuous compounds via associated scaffolds. This analysis reveals that only substances **3** and **10** have  $p$  scores higher than 300.

Interestingly, the calculated log D of substances **3** and **10** indicates the lowest lipophilicity index, thus should have the lowest permeability into cells. There was no correlation between the log D and LUMO energies ( $R^2 = 0.0107$ ) or log D and electrophilicity ( $R^2 = 0.1575$ ) of all substances. Thus, for the investigated series of substances, the log D–LUMO relationship is not an indicator of



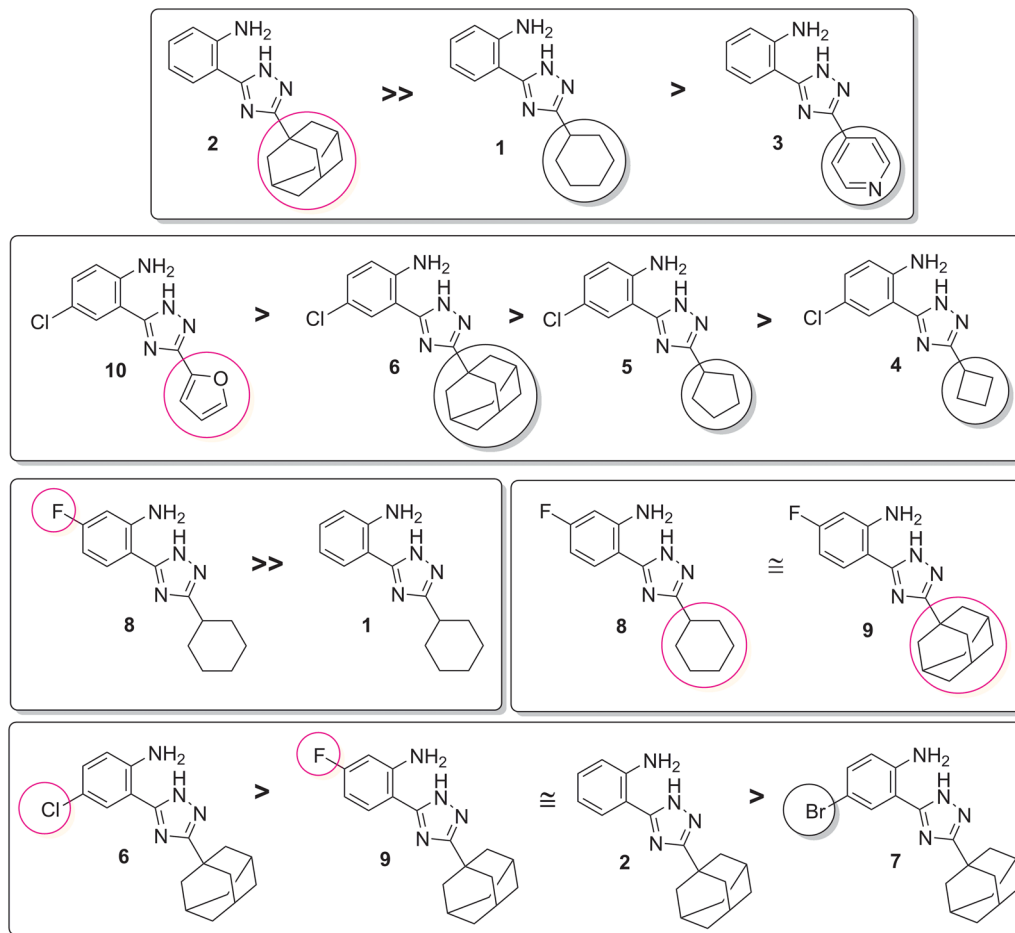


**FIGURE 5** The structure–activity relationship of investigated triazoles **1–10** in order of decreasing activities (averages from Table 2)

mutagenicity. Besides this, an elevated level of potential carcinogenicity of substances may be expected from the calculated high values of electrophilicity. However, as discussed by Tiwary et al.<sup>[42]</sup> flavonoids interacting with DNA confer prooxidative stress, which, in turn, results in positive mutagenic activity in the reverse *Salmonella* mutagenicity test. Nevertheless, with respect to transformation to cancer cells, flavonoids act protectively on mammalian organisms. Also, Gopalakrishnan et al.<sup>[43]</sup> calculated electrophilicity of silymarin as 3.24 eV, which is above that of the substances presented here. However, it was also demonstrated that silibinin, a major active component of silymarin, can form complexes with DNA, and at the same time confer radioprotective and anticancer activity. Thus, the electrophilic profile of molecules may give a strong indication towards reactivity with DNA; with consideration to carcinogenicity the interrelation may be less straightforward and correspondingly interpretation of data should not be overstressed.

Recently, Gadaleta et al.<sup>[44]</sup> reported on a knowledge-based classification algorithm, which implemented a series of defined rules to predict the mutagenic potency of aromatic amines. Applying these rules, the 1,2,4-triazole compounds presented here should be nonmutagens. Namely, a possible metabolization consists of *N*-oxidation of the amine group to *N*-hydroxylamine mediated by

cytochrome P-450,<sup>[45]</sup> followed by an enzymatic acetylation or sulfonation, which further leads to the formation of a nitrenium ion. This highly reactive electrophilic species could bind covalently to biomacromolecules-generating aminoaryl derivatives.<sup>[46]</sup> *N*-Hydroxylamines also could be metabolically converted to nitroso species leading to the formation of reactive oxygen species. The level of mutagenicity is also related to the degree of oxidizability of the amino group and the stability of the generated nitrenium ion.<sup>[45]</sup> The electron-withdrawing groups destabilize the nitrenium ion, reducing the mutagenic potential of the parent amine. So, substance **3** with the pyridine-3-yl substituent and **10** with furan-3-yl should have the lowest mutagenic potential. On the contrary, it was found that electron-donating (ED) groups as *para*-alkyl substituents increase mutagenic activity by stabilization of the nitrenium ion. In addition, the elongation of alkyl substituents up to adamantyl should increase their mutagenic activity. But for larger substituents, especially in the *ortho*-position, such as the bulky 1,2,4-triazole ring, the mutagenicity of anilines primarily depends on steric effects<sup>[47]</sup> leading to less toxic compounds. Moreover, aromatic amines with more than one ring forming a conjugated system, either fused or nonfused, showed greater mutagenic activity by charge delocalization, but not stabilization of nitrenium species.<sup>[48]</sup>

**TABLE 5** Mutagenicity index ( $M_i$ ) calculated for reference mutagens and investigated substances relative to negative control plates with 100  $\mu$ l of DMSO (dimethylsulfoxide)<sup>[18]</sup>

Substances	Dose (µg/ plate)	TA 98		TA 100	
		+S9-mix		+S9-mix	
2-Nitrofluorene	10	58.40			
Methyl methansulfonate	1	4.20			
2-Aminofluorene	10	1.56	47.35	1.01	4.58
Hymexazol	50	0.71	0.85	1.03	0.90
1	50	0.76	0.88	0.98	0.87
2	50	1.04	0.87	1.00	1.07
3	50	0.81	0.63	0.91	0.94
4	50	1.19	0.72	1.14	1.08
5	50	1.21	0.77	0.89	0.92
6	50	1.17	0.79	1.02	0.81
7	50	1.07	0.95	0.87	1.23
8	50	0.90	0.51	0.97	0.81
9	50	1.04	0.91	1.06	0.75
10	50	1.48	2.52	1.28	2.79

## 2.4.2 | Ames gene-toxicity test

So, to examine the above-predicted characteristics, substances were tested for mutagenicity by a standard plate incorporation assay with *Salmonella typhimurium* strains TA98 and TA100, as described by Maron and Ames (Table 5).<sup>[22,35]</sup>

The assay was carried out with and without addition of rat liver S9 extract for metabolic activation. According to the number of formed revertants, the studied substances were found to be nonmutagenic (mutagenicity index [ $M_i$ ], <2), except substance 10. Only this triazole showed an elevated  $M_i$  when tested at

50  $\mu$ g/plate with metabolic activation, which was at 2.52 and 2.79 for strain TA98 and TA100, respectively. Increasing the dose to 500  $\mu$ g per plate resulted in a  $M_i$  of 10.33 for TA98 with metabolic activation. These data reveal the mutagenic potential of substance 10. Nevertheless, compared to the reference substance 2-amino-fluorene ( $M_i$  = 47.35 [TA98] and 4.58 [TA100]; 10  $\mu$ g/plate; metabolic activation), the mutagenicity is quite weak. Only substance 10 was significantly activated by S9-mix cytochrome P-450. The elevated mutagenicity of substance 10 may be caused by the enzymatic oxidation of the amino group, but also by the presence of the furan-3-yl ring. This structure is prone to reversibly intercalate into the DNA and thereby introduce base pair mutations in the course of DNA-replication. According to the highest negative charges calculated by HyperChem 8.0 (Supporting Information), the most probable centers for electrophilic attacks are nitrogens in  $NH_2$ -groups of substances 3 (−0.376) and 10 (−0.369). Considering the in vitro nonmutagenicity of substance 3, it is obvious that not only the heterocyclic substituent but also steric effects contribute to the elevated mutagenicity potential of substance 10.<sup>[47]</sup> Generally, it has to be considered that the prokaryotic in vitro Ames assay reflects in vivo mutagenicity and carcinogenicity in eukaryotic organisms only to a certain degree: DNA repair capacities, distribution and apparent concentration levels of substances and metabolic conversions are unknowns, which can only be studied by animal experiments.

## 2.4.3 | Drug-likeness calculations

Bioavailability of drug candidates is an important parameter to evaluate the safety of chemicals. Thus, drug-likeness parameters of novel triazoles 1–10 and hymexazol were calculated with the Molinspiration online engine.<sup>[35]</sup> All substances complied to drug-likeness relevant descriptors such as molecular weight (MW),

**TABLE 6** Calculated parameters of drug-likeness optimization of triazoles 1–10 and hymexazol (hym)

Compound no.	SMILES	MW	miLogP	TPSA	HBA	HBD	nrotb
hym	<chem>CC1=CC(=NO1)O</chem>	99.1	0.55	46.3	3	1	0
1	<chem>NC1=CC=CC=C1C2=NC(=N[NH]2)C3CCCCC3</chem>	242.33	2.94	67.6	4	3	2
2	<chem>NC1=CC=C(C1C2=NC(=N[NH]2)[C]34CC5[CH2][CH](C[CH]([CH2]5)C3)C4</chem>	294.40	3.96	67.6	4	3	2
3	<chem>NC1=CC=CC=C1C2=NC(=N[NH]2)C3=CC=CN=C3</chem>	237.27	1.99	80.5	5	3	2
4	<chem>NC1=CC=C(C1C2=NC(=N[NH]2)C3CCCC3</chem>	248.72	2.35	67.6	4	3	2
5	<chem>NC1=CC=C(C1C2=NC(=N[NH]2)C3CCCC3</chem>	262.74	3.08	67.6	4	3	2
6	<chem>NC1=CC=C(C1C2=NC(=N[NH]2)[C]34CC5[CH2][CH](C[CH]([CH2]5)C3)C4</chem>	328.85	4.61	67.6	4	3	2
7	<chem>NC1=CC=C(Br)C=C1C2=NC(=N[NH]2)[C]34CC5[CH2][CH](C[CH]([CH2]5)C3)C4</chem>	373.30	4.74	67.6	4	3	2
8	<chem>NC1=CC(=CC=C1C2=NC(=N[NH]2)C3CCCCC3)F</chem>	260.32	3.08	67.6	4	3	2
9	<chem>NC1=CC(=CC=C1C2=NC(=N[NH]2)[C]34CC5[CH2][CH](C[CH]([CH2]5)C3)C4)F</chem>	312.39	4.09	67.6	4	3	2
10	<chem>NC1=CC=C(C1C2=NC(=N[NH]2)C3=COC=C3</chem>	260.68	2.66	80.7	5	3	2
Drug lead-like criteria		≤500	≤5	≤140	≤10	≤5	≤10

Abbreviations: HBA, hydrogen bond acceptors; HBD, hydrogen bond donors; MW, molecular weight; miLogP, octanol/water partition coefficient; nrotb, number of rotatable bonds; TPSA, molecular topological polar surface area.

**TABLE 7** Correlation coefficients between average antifungal activity of triazoles **1–10** and their calculated *miLogP*, *Log D*, and affinity to the enzymatic targets

	MW	TPSA	<i>miLogP</i>	Log D at pH			
				2	4	7.5	9
<i>R</i> <sup>2</sup>	0.0549	0.0132	0.1349	0.3965	0.2048	0.1835	0.3066
Towards affinity to enzymes							
		CYP51	NMT	SAP2	Topo II	MurD	GlcN-6-P
<i>R</i> <sup>2</sup>		0.0199	0.0099	0.0572	0.1368	0	0.0476

Abbreviations: CYP51, affinity to 14 $\alpha$ -demethylase; GlcN-6-P, L-glutamine:D-fructose-6-phosphate aminotransferase; *Log D*, distribution coefficient; *miLogP*, octanol/water partition coefficient; MurD, UDP-*N*-acetyl-muramoyl-L-alanine:D-glutamate ligase; MW, molecular weight; NMT, *N*-myristoyl-transferase; SAP2, secreted aspartic proteinase; Topo II, topoisomerase II; TPSA, molecular topological polar surface area.

octanol/water partition coefficient, hydrogen bond acceptors and donors as well as number of rotatable bonds (Table 6).

Molecular topological polar surface areas (TPSA) were calculated to be not more than 140 Å<sup>2</sup>, but lower than 75 Å<sup>2</sup> for all substances except the **3rd**, so they could possibly penetrate the blood–brain barrier. Also, substances **2**, **6**, and **9** had good lipophilicity and low TPSA. Still their molecular surfaces were larger than that of hymexazol, which is already widely used as a pesticide with no detected mammalian toxicology.<sup>[49]</sup>

#### 2.4.4 | Correlations between calculated descriptors

To analyze what descriptor had a higher possibility to affect penetration of triazoles into the fungal cell and bind to the enzymatic target, we calculated the correlation coefficients between average antifungal activity of each tested substance and its several found parameters (Table 7).

The strongest correlation (0.3965) was found between antifungal activity and *Log D* at pH 2. Therefore, acidification of the fungal growth media, when treated with substances could increase their level of activity and avoid one of the fungal resistance mechanisms. However, deprotonation at pH 9 also had a positive impact on correlation with *R*<sup>2</sup> = 0.3066. Interestingly, correlation with MW was better than with TPSA, still with very low values. Among the affected target enzymes, topoisomerase II (Topo II, *R*<sup>2</sup> = 0.1368) was found with a higher calculated probability to be involved in inhibition of all tested fungal strains.

### 3 | CONCLUSION

We identified several antifungal agents of phytopathogenic significance among the novel series of 1,2,4-triazole derivatives, bearing bulky alkyl, heterocyclic, and halogen substituents. With respect to toxicology, our data so far show no restrictive risk. Calculated drug-likeness parameters suggest a good bioavailability of the substances with low toxicity. 14- $\alpha$ -Demethylase and *N*-myristoyltransferase are suggested to be the most probable enzymes for binding. Considering the shown nonmutagenicity of {2-(3-*R*-1*H*-1,2,4-triazol-5-yl)phenyl}-amines, they warrant further investigations of their antifungal

potential and ecotoxicology profile to be developed into useful agrochemicals.

## 4 | EXPERIMENTAL

### 4.1 | Chemistry

#### 4.1.1 | General

Melting points were determined in open capillary tubes and were uncorrected. The elemental analyses (C, H, N, and S) were performed using a Vario EL Cube analyzer (Elementar Americas, NJ). Analyses were indicated by the symbols of the elements or functions within  $\pm 0.3\%$  of the theoretical values. The <sup>1</sup>H NMR spectra (400 MHz) and <sup>13</sup>C NMR spectra (125 MHz) were recorded on a Varian-Mercury 400 (Varian Inc., Palo Alto, CA) spectrometer with TMS as an internal standard in DMSO-*d*<sub>6</sub> solution. LC–MS were recorded using the chromatography/mass spectrometric system consisting of an “Agilent 1100 Series” high-performance liquid chromatograph (Agilent, Palo Alto, CA) equipped with an “Agilent LC/MSD SL” diode matrix.

Synthesis of starting substances (**b–g**, Figure 2) was done using the prior reported methods.<sup>[23–31]</sup> LC–MS and <sup>1</sup>H NMR spectra of **1–10** are presented in Supporting Information.

The InChI codes of the investigated compounds together with some biological activity data are also provided as Supporting Information.

#### 2-(3-Cyclohexyl-1*H*-1,2,4-triazol-5-yl)aniline (**1**)

Yield, 93.2%. M.p. 152–154°C; <sup>1</sup>H NMR:  $\delta$ , ppm. (*J*, Hz): 13.53/13.37 (b.s, 1H, NH), 7.92/7.62 (unres.d, 1H, H-3), 6.99 (unres.t, 1H, H-5), 6.68 (unres.t, 1H, H-4), 6.48–6.58 (m, 1H, H-6), 6.17 (b.s, 2H, NH<sub>2</sub>), 2.83–2.65 (m, 1H, H-1 cyclohexane), 2.17–1.15 (m, 10H, H-2,2, 3,3, 4,4, 5,5, 6,6 cyclohexane); <sup>13</sup>C NMR:  $\delta$ , ppm: 160.7 (triazole C-3), 155.0 (triazole C-5), 147.1 (Ar C-1), 130.0 (Ar C-3), 128.0 (Ar C-5), 116.2 (Ar C-4), 115.6 (Ar C-2,6), 36.2 (Cy C-1), 31.6 (Cy C-2, 6), 26.0 (Cy C-4), and 25.8 (Cy C-3,5); LC–MS, *m/z* = 285 [M+1]; Anal. calcd. for C<sub>14</sub>H<sub>18</sub>N<sub>4</sub>: C, 69.39; H, 7.49; N, 23.12; Found: C, 69.36; H, 7.50; N, 23.13.

**2-(3-(Adamantan-1-yl)-1H-1,2,4-triazol-5-yl)aniline (2)**

Yield: 89.3%. M.p. 150–152°C;  $^1\text{H}$  NMR:  $\delta$ , ppm. (J, Hz): 13.58/13.23 (b.s, 1H, NH), 7.98/7.54 (unres.d, 1H, H-3), 7.00 (unres.t, 1H, H-5), 6.70 (unres.t, 1H, H-4), 6.58–6.45 (m, 1H, H-6), 6.19 (b.s, 2H,  $\text{NH}_2$ ), 2.12–1.98 (m, 9H, Ad), 1.85–1.74 (m, 6H, Ad);  $^{13}\text{C}$  NMR:  $\delta$ , ppm: 163.7 (triazole C-3), 161.3 (triazole C-5), 146.9 (Ar C-1), 130.8/129.6 (Ar C-3), 128.4/127.1 (Ar C-5), 116.0 (Ar C-4), 115.6 (Ar C-2), 113.6 (Ar C-6), 41.7 (Ad C-1), 41.1 (Ad C-2,8,9), 36.8/36.5 (Ad C-4,6,10), and 28.3/28.1 (Ad C-3,5,7); LC-MS,  $m/z$  = 295 [M+1]; Anal. calcd. for  $\text{C}_{18}\text{H}_{22}\text{N}_4$ : C, 73.44; H, 7.53; N, 19.03; Found: C, 73.42; H, 7.54; N, 19.04.

**2-(3-(Pyridin-3-yl)-1H-1,2,4-triazol-5-yl)aniline (3)**

Yield: 95.9%. M.p. 247–249°C;  $^1\text{H}$  NMR,  $\delta$ , ppm. (J, Hz): 14.54/14.10 (b.s, 1H, NH), 9.26 (s, 1H, H-2 Pyr), 8.58 (d,  $J$  = 8.0 Hz, 1H, H-6 Pyr), 8.39 (d,  $J$  = 7.9 Hz, 1H, H-4 Pyr), 7.72 (d,  $J$  = 7.9 Hz, 1H, H-3), 7.41 (t,  $J$  = 7.6 Hz, 1H, H-5 Pyr), 7.11 (t,  $J$  = 7.7 Hz, 1H, H-5), 6.88–6.51 (m, 2H, H-4, H-6), 6.26 (b.s, 2H,  $\text{NH}_2$ );  $^{13}\text{C}$  NMR:  $\delta$ , ppm: 157.1 (triazole C-3), 150.6 (triazole C-5), 147.6 (Pyr C-4), 147.5 (Ar C-1, Pyr C-2), 133.8 (Pyr C-6), 131.3 (Ar C-3), 127.6 (Ar C-5), 124.4 (Pyr C-1,5), 116.7 (Ar C-4), and 115.7 (Ar C-2,6); LC-MS,  $m/z$  = 238 [M+1]; Anal. calcd. for  $\text{C}_{13}\text{H}_{11}\text{N}_5$ : C, 65.81; H, 4.67; N, 29.52; Found: C, 65.80; H, 4.68; N, 29.51.

**4-Chloro-2-(3-cyclobutyl-1H-1,2,4-triazol-5-yl)aniline (4)**

Yield: 88.7%. M.p. 176–178°C;  $^1\text{H}$  NMR:  $\delta$ , ppm. (J, Hz): 13.70/13.43 (b.s, 1H, NH), 7.97/7.68 (unres.d, 1H, H-3), 6.96 (d,  $J$  = 8.7 Hz, 1H, H-5), 6.72 (d,  $J$  = 8.6 Hz, 1H, H-6), 6.33 (b.s, 2H,  $\text{NH}_2$ ), 3.78–3.52 (m, 1H, H-1 cyclobutane), 2.47–2.30 (m,  $J$  = 18.0 Hz, 4H, H-2,2, 4,4 cyclobutane), 2.05 (dt,  $J$  = 19.6, 10.4 Hz, 2H, H-3,3 cyclobutane);  $^{13}\text{C}$  NMR:  $\delta$ , ppm: 160.6 (triazole C-3), 159.7 (triazole C-5), 145.8 (Ar C-1), 130.7/129.3 (Ar C-3), 127.2/126.2 (Ar C-5), 118.8 (Ar C-4), 117.7 (Ar C-2), 114.5 (Ar C-6), 31.6 (cyclobutane C-1), 28.0 (cyclobutane C-2,4), and 18.7 (cyclobutane C-3); LC-MS,  $m/z$  = 249 [M+1]; Anal. calcd. for  $\text{C}_{12}\text{H}_{13}\text{ClN}_4$ : C, 57.95; H, 5.27; Cl, 14.25; N, 22.53; Found: C, 57.93; H, 5.29; Cl, 14.27; N, 22.52.

**4-Chloro-2-(3-cyclopentyl-1H-1,2,4-triazol-5-yl)aniline (5)**

Yield: 85.5%. M.p. 161–163°C;  $^1\text{H}$  NMR:  $\delta$ , ppm. (J, Hz): 13.51 (s, 1H, NH), 7.88 (s, 1H, H-3), 6.96 (d,  $J$  = 8.6 Hz, 1H, H-5), 6.72 (d,  $J$  = 8.8 Hz, 1H, H-6), 6.33 (b.s, 2H,  $\text{NH}_2$ ), 3.21 (t,  $J$  = 8.4 Hz, 1H, H-1 cyclopropane), 2.19–1.51 (m, 8H, H-2,2 3,3, 4,4, 5,5 cyclopropane);  $^{13}\text{C}$  NMR:  $\delta$ , ppm: 160.5 (triazole C-3, C-5), 145.8 (Ar C-1), 130.6/129.2 (Ar C-3), 127.2/126.2 (Ar C-5), 118.8 (Ar C-4), 117.7 (Ar C-2), 114.6 (Ar C-6), 36.8 (cyclopentan C-1), 32.2 (cyclopentan C-2, 5), 25.4 (cyclopentan C-3,4); LC-MS,  $m/z$  = 263 [M+1]; Anal. calcd. for  $\text{C}_{13}\text{H}_{15}\text{ClN}_4$ : C, 59.43; H, 5.75; Cl, 13.49; N, 21.32; Found: C, 59.42; H, 5.76; Cl, 13.50; N, 21.31.

**2-(3-(Adamantan-1-yl)-1H-1,2,4-triazol-5-yl)-4-chloroaniline (6)**

Yield: 83.1%. M.p. 256–258°C;  $^1\text{H}$  NMR:  $\delta$ , ppm. (J, Hz): 13.65/13.40 (b.s, 1H, NH), 7.90 (s, 1H, H-3), 6.95 (d,  $J$  = 8.6 Hz, 1H, H-5), 6.71 (d,  $J$  = 8.9 Hz, 1H, H-6), 6.32 (b.s, 2H,  $\text{NH}_2$ ), 2.14–1.98 (m, 9H, Ad), 1.79 (s, 6H, Ad);  $^{13}\text{C}$  NMR:  $\delta$ , ppm: 164.1 (triazole C-3), 160.1 (triazole

C-5), 145.9 (Ar C-1), 129.3 (Ar C-3), 127.1 (Ar C-5), 118.8 (Ar C-4), 117.7 (Ar C-2,6), 41.1 (Ad C-1,2,8,9), 36.5 (Ad C-4,6,10), and 28.1 (Ad C-3,5,7); LC-MS,  $m/z$  = 329 [M+1]; Anal. calcd. for  $\text{C}_{18}\text{H}_{21}\text{ClN}_4$ : C, 65.74; H, 6.44; Cl, 10.78; N, 17.04; Found: C, 65.72; H, 6.45; Cl, 10.79; N, 17.03.

**2-(3-(Adamantan-1-yl)-1H-1,2,4-triazol-5-yl)-4-bromoaniline (7)**

Yield: 88.9%. M.p. 249–251°C;  $^1\text{H}$  NMR:  $\delta$ , ppm. (J, Hz): 13.55/13.35 (b.s, 1H, NH), 8.01 (s, 1H, H-3), 7.07 (d,  $J$  = 8.6 Hz, 1H, H-5), 6.68 (d,  $J$  = 8.7 Hz, 1H, H-6), 6.36 (b.s, 2H,  $\text{NH}_2$ ), 2.13–1.98 (m, 9H, Ad), 1.80 (s, 6H, Ad); LC-MS,  $m/z$  = 374 [M+1]; Anal. calcd. for  $\text{C}_{18}\text{H}_{21}\text{BrN}_4$ : C, 57.92; H, 5.67; Br, 21.40; N, 15.01; Found: C, 57.90; H, 5.68; Br, 21.41; N, 15.01.

**2-(3-Cyclohexyl-1H-1,2,4-triazol-5-yl)-5-fluoroaniline (8)**

Yield: 97.9%. M.p. 151–153°C;  $^1\text{H}$  NMR:  $\delta$ , ppm. (J, Hz): 13.55/13.28 (b.s, 1H, NH), 7.96/7.59 (unres.d, 1H, H-3), 6.66–6.33 (m, 3H, H-6,  $\text{NH}_2$ ), 6.26 (d,  $J$  = 8.9 Hz, 1H, H-4), 2.85–2.63 (m, 1H, H-1 cyclohexane), 2.08–1.75 (m, 4H, H-2,2, 6,6 cyclohexane), 1.74–1.23 (m, 6H, H-3,3, 4,4, 5,5 cyclohexane);  $^{13}\text{C}$  NMR:  $\delta$ , ppm: 163.5 (d,  $J$  = 242.3 Hz, Ar C-5), 160.8 (triazole C-3), 160.4 (triazole C-5), 148.9 (d,  $J$  = 10.4 Hz, Ar C-1), 130.2 (d,  $J$  = 10.6 Hz, Ar C-3), 110.2 (Ar C-2), 102.5 (d,  $J$  = 23.7 Hz, Ar C-4), 101.3 (d,  $J$  = 24.0 Hz, Ar C-6), 35.7 (Cy C-1), 31.4 (Cy C-2,6), 25.8 (Cyc C-4), and 25.7 (Cyc C-3,5); LC-MS,  $m/z$  = 261 [M+1]; Anal. calcd. for  $\text{C}_{14}\text{H}_{17}\text{FN}_4$ : C, 64.60; H, 6.58; F, 7.30; N, 21.52; Found: C, 64.59; H, 6.58; F, 7.31; N, 21.50.

**2-(3-(Adamantan-1-yl)-1H-1,2,4-triazol-5-yl)-5-fluoroaniline (9)**

Yield: 95.2%. M.p. 224–226°C;  $^1\text{H}$  NMR:  $\delta$ , ppm. (J, Hz): 13.33 (s, 1H, NH), 7.98/7.60 (unres.d, 1H, H-3), 6.60–6.35 (m, 3H, H-6,  $\text{NH}_2$ ), 6.23 (d,  $J$  = 8.7 Hz, 1H, H-4), 2.13–1.96 (m, H, Ad), 1.79 (s, 6H, Ad);  $^{13}\text{C}$  NMR:  $\delta$ , ppm: 164.6 (triazole C-3), 163.9 (triazole C-5), 161.6 (d,  $J$  = 256.0 Hz, Ar C-5), 149.0 (d,  $J$  = 14.4 Hz, Ar C-1), 130.3 (Ar C-6), 110.4 (Ar C-1), 102.5 (d,  $J$  = 25.6 Hz, Ar C-6), 101.4 (d,  $J$  = 24.1 Hz, Ar C-4), 41.1 (Ad C-1,2,8,9), 36.5 (Ad C-4,6,10), and 28.1 (Ad C-3,5,7); LC-MS,  $m/z$  = 313 [M+1]; Anal. calcd. for  $\text{C}_{18}\text{H}_{21}\text{FN}_4$ : C, 69.21; H, 6.78; F, 6.08; N, 17.94; Found: C, 69.20; H, 6.79; F, 6.06; N, 17.96.

**4-Chloro-2-(3-(furan-3-yl)-1H-1,2,4-triazol-5-yl)aniline (10)**

Yield 97.9%. M.p. 248–250°C;  $^1\text{H}$  NMR:  $\delta$ , ppm. (J, Hz): 14.20/13.98 (b.s, 1H, NH), 8.31–7.52 (m, 3H, H-3, furan H-2, furan H-5), 7.10–6.68 (m, 3H, H-4, H-5, furan H-4), 6.38 (b.s, 2H,  $\text{NH}_2$ );  $^{13}\text{C}$  NMR:  $\delta$ , ppm: (126 MHz, DMSO- $d_6$ )  $\delta$  161.3 (triazole C-3), 148.7 (triazole C-5), 147.0/146.0 (Ar C-1), 145.3/144.6 (furan C-2), 143.1/142.1 (furan C-5), 131.0/129.6 (Ar C-3), 127.3/126.4 (Ar C-5), 118.9 (Ar C-4), 118.4 (Ar C-2), 117.8 (Ar C-6), 109.0 (furan C-3,4); LC-MS,  $m/z$  = 261 [M+1]; Anal. calcd. for  $\text{C}_{12}\text{H}_9\text{ClN}_4\text{O}$ : C, 55.29; H, 3.48; Cl, 13.60; N, 21.49; O, 6.14; Found: C, 55.27; H, 3.49; Cl, 13.61; N, 21.47; O, 6.15.

## 4.2 | Antifungal studies

The mycelial growth rate assay was used for antifungal studies.<sup>[14]</sup> Strains of filamentous fungi were obtained from the following

sources: *A. niger* DSM 246, *G. graminis* DSM 12044, *C. purpurea* DSM 715, *C. coccodes* DSM 2492, *A. alternata* DSM 1102, *F. graminearum* DSM 1095, *F. fujikuroi* DSM 893, *V. lecanii* DSM 63098, *M. indicus* DSM 2185, and *P. digitatum* DSM 2731 from DSMZ (Braunschweig, Germany); *F. oxysporum* 39/1201 St. 9336, *B. cinerea* from the Technische Universität Berlin (Germany); *Phytophthora infestans* (GL-1 01/14 wild strain), p-3 (4/91; R+) and p-4 (4/91; R-) strains were kindly donated by Julius Kühn-Institut (Quedlinburg, Germany); *C. higginsianum* (MAFF 305635), originally isolated by the Ministry of Agriculture, Forest and Fisheries collection, Japan, via the Department of Biology, Friedrich Alexander Universität (Erlangen, Germany). PDA was purchased from C. Roth (Karlsruhe, Germany). Hymexazol (98%) was obtained from Prosperity World Store (Hebei, China). The procedure was used as described earlier.<sup>[35]</sup>

### 4.3 | Other methods

Molecular docking studies, quantum data, molecular descriptors calculations and the *Salmonella* reverse-mutagenicity test were done as described earlier.<sup>[35]</sup>

### ACKNOWLEDGMENTS

Authors gratefully acknowledge Enamine Ltd. (Kiev, Ukraine) and the German Federal Ministry of Education and Research (Grant: FKZ 03FH025IX4) for financial support for this study; the Federal Research Centre for Cultivated Plants (Quedlinburg, Germany) for providing the strain *P. infestans*; the Department of Biology, Friedrich Alexander University, Erlangen, Nürnberg, Germany for the strain *Colletotrichum higginsianum*, and Dr. Oleksii Antypenko (Zaporizhzhya State Medical University, Ukraine) for conducting molecular docking.

### CONFLICT OF INTERESTS

The authors declare that there are no conflict of interests.

### AUTHOR CONTRIBUTION

All authors contributed equally.

### ORCID

Lyudmyla Antypenko  <http://orcid.org/0000-0003-0057-1551>

Zhanar Sadykova  <http://orcid.org/0000-0002-4807-9008>

Kostiantyn Shabelnyk  <http://orcid.org/0000-0003-2008-8380>

Sergiy Kovalenko  <http://orcid.org/0000-0001-8017-9108>

### REFERENCES

- [1] V. Meyer, M. R. Andersen, A. A. Brakhage, G. H. Braus, M. X. Caddick, T. C. Cairns, R. P. de Vries, T. Haarmann, K. Hansen, C. Hertz-Fowler, S. Krappmann, U. H. Mortensen, M. A. Peñalva, A. F. J. Ram, R. M. Head, *Fungal Biol. Biotechnol.* **2016**, 3, 6. <https://doi.org/10.1186/s40694-016-0024-8>
- [2] S. Campoy, J. L. Adrio, *Biochem. Pharmacol.* **2017**, 133, 86.
- [3] F. J. Schwinn, *Pestic. Sci.* **1984**, 15, 40. <https://doi.org/10.1002/ps.2780150107>
- [4] J. E. Parker, A. G. S. Warrilow, C. L. Price, J. G. L. Mullins, D. E. Kelly, S. L. Kelly, *J. Chem. Biol.* **2014**, 7, 143.
- [5] C. A. Hitchcock, K. Dickinson, S. B. Brown, E. G. V. Evans, D. J. Adams, *Biochem. J.* **1990**, 266, 475.
- [6] B. C. Monk, T. M. Tomasiak, M. V. Keniya, F. U. Huschmann, J. D. A. Tyndall, J. D. O'Connell, R. D. Cannon, J. G. McDonald, A. Rodriguez, J. S. Finer-Moore, R. M. Stroud, *Proc. Natl. Acad. Sci. USA* **2014**, 111, 3865.
- [7] A. H. Fairlamb, N. A. R. Gow, K. R. Matthews, A. P. Waters, *Nat. Microbiol.* **2016**, 1, 1. <https://doi.org/10.1038/nmicrobiol.2016.92>
- [8] S. Berger, Y. El Chazli, A. F. Babu, A. T. Coste, *Front. Microbiol.* **2017**, 8, 1. <https://doi.org/10.3389/fmicb.2017.01024>
- [9] A. Chowdhary, S. Kathuria, J. Xu, J. F. Meis, *PLOS Pathog.* **2013**, 9, 1. <https://doi.org/10.1371/journal.ppat.1003633>
- [10] A. A. Sagatova, M. V. Keniya, R. K. Wilson, M. Sabherwal, J. D. A. Tyndall, B. C. Monk, *Sci. Rep.* **2016**, 6, 1. <https://doi.org/10.1038/srep26213>
- [11] J. R. Perfect, *Exp. Opin. Emerg. Drugs* **2016**, 21, 129.
- [12] W. Zhang, G. Sui, Y. Li, M. Fang, X. Yang, X. Ma, W. Zhou, *Chem. Pharm. Bull.* **2016**, 64, 616.
- [13] G. S. Basarab, M. Pifferitti, M. M. Bolinski, *Pestic. Sci.* **1991**, 31, 403. <https://doi.org/10.1002/ps.2780310402>
- [14] R. Tang, L. Jin, C. Mou, J. Yin, S. Bai, D. Hu, J. Wu, S. Yang, B. Song, *Chem. Central J.* **2013**, 7, 1. <https://doi.org/10.1186/1752-153X-7-30>
- [15] V. M. Odyntsova, *Curr. Issues Pharm. Med.: Sci. Pract.* **2016**, 3, 49. <https://doi.org/10.14739/2409-2932.2016.3.77945>
- [16] V. M. Odyntsova, A. M. Kamyshny, N. N. Polischuk, *Curr. Issues Pharm. Med.: Sci. Pract.* **2017**, 3, 264. <https://doi.org/10.14739/2409-2932.2017.3.112756>
- [17] G.-S. Lin, W.-G. Duan, L.-X. Yang, M. Huang, F.-H. Lei, *Molecules* **2017**, 22, 193. <https://doi.org/10.3390/molecules22020193>
- [18] S. M. Somagond, R. R. Kamble, P. P. Kattimani, S. D. Joshi, S. R. Dixit, *Heterocycl. Commun.* **2017**, 23, 317. <https://doi.org/10.1515/hc-2016-0073>
- [19] R. L. Lopez de Compadre, A. K. Debnath, A. J. Shusterman, C. Hansch, *Environ. Mol. Mutagen.* **1990**, 15, 44. <https://doi.org/10.1002/em.2850150107>
- [20] V. André, C. Boissart, F. Sichel, P. Gauduchon, J. Y. Le Talaër, J. C. Lancelot, C. Mercier, S. Chemtob, E. Raoult, A. Tallec, *Mutat. Res. Genet. Toxicol. Environ. Mutagen.* **1997**, 389, 247. [https://doi.org/10.1016/S1383-5718\(96\)00155-6](https://doi.org/10.1016/S1383-5718(96)00155-6)
- [21] T. Takamura-Enya, H. Suzuki, Y. Hisamatsu, *Mutagenesis* **2006**, 21, 399. <https://doi.org/10.1093/mutage/gel045>
- [22] D. M. Maron, B. N. Ames, *Mutat. Res.* **1983**, 113, 173.
- [23] M. J. Kornet, T. Varia, W. Beaven, *J. Heterocycl. Chem.* **1983**, 20, 1553.
- [24] W. L. F. Armarego, *J. Appl. Chem.* **1961**, 11, 70.
- [25] G.-F. Xu, B.-A. Song, P. S. Bhadury, S. Yang, P. Q. Zhang, L. H. Jin, W. Xue, D. Y. Hu, P. Lu, *Bioorg. Med. Chem.* **2007**, 15, 3768.
- [26] M. Claesen, H. Vanderhaeghe, *Bull. Soc. Chim. Belges* **1959**, 68, 220.
- [27] K. P. Schabelnyk, S. V. Kholodnyak, G. G. Berest, S. I. Kovalenko, N. M. Polishchuk, A. M. Kamyshnyi, *Zaporozhye Med. J.* **2018**, 20, 425. <https://doi.org/10.14739/2310-1>
- [28] O. V. Karpenko, S. I. Kovalenko, *Zhurnal orhanichnoyi ta farmatsevtichnoyi khimiyi* **2005**, 2, 47.
- [29] O. V. Karpenko, S. I. Kovalenko, *Zhurnal orhanichnoyi ta farmatsevtichnoyi khimiyi* **2005**, 4, 61.
- [30] O. V. Karpenko, S. I. Kovalenko, *Zhurnal orhanichnoyi ta farmatsevtichnoyi khimiyi* **2006**, 2, 65.
- [31] S. I. Kovalenko, *Sci. Pharm.* **2013**, 81, 359. <https://doi.org/10.3797/scipharm.1211-08>



- [32] S. V. Kholodnyak, K. P. Schabelnyk, G. O. Shernova, S. I. Kovalenko, S. D. Trshetsinskij, T. Y. Sergeieva, S. I. Okovytyy, S. V. Shishkina, *News Pharm.* **2015**, 3, 9.
- [33] T. Sergeieva, M. Bilichenko, S. Holodnyak, Y. V. Monaykina, S. I. Okovytyy, S. I. Kovalenko, E. Voronkov, J. Leszczynski, *J. Phys. Chem A.* **2016**, 120, 10116.
- [34] O. M. Antypenko, S. I. Kovalenko, O. V. Karpenko, *Syn. Commun.* **2016**, 46, 551. <https://doi.org/10.1080/00397911.2016.1156131>
- [35] L. Antypenko, F. Meyer, O. Kholodniak, Z. Sadykova, T. Jirásková, A. Troianova, V. Buhaiova, S. Cao, S. Kovalenko, L.-A. Garbe, K. G. Steffens, *Arch. Pharm. Chem. Life Sci.* **2018**, 352, 1. <https://doi.org/10.1002/ardp.201800275>
- [36] T. Y. Hargrove, L. Friggeri, Z. Wawrzak, S. Sivakumaran, E. M. Yazlovitskaya, S. W. Hiebert, F. P. Guengerich, M. R. Waterman, G. I. Lepesheva, *J. Lipid Res.* **2016**, 57, 1552.
- [37] C. Lass-Flörl, *Drugs* **2011**, 71, 2405.
- [38] T. Bagar, K. Altenbach, N. D. Read, M. Benčina, *Eukaryotic Cell* **2009**, 8, 703. <https://doi.org/10.1128/EC.00333-08>
- [39] C. S. Danby, D. Boikov, R. Rautemaa-Richardson, J. D. Sobel, *Antimicrob. Agents Chemother.* **2012**, 56, 1403. <https://doi.org/10.1128/AAC.05025-11>
- [40] A. Ullah, M. I. Lopes, S. Brul, G. J. Smits, *Microbiology* **2013**, 159, 803. <https://doi.org/10.1099/mic.0.063610-0>
- [41] O. Rivero-Menendez, A. Alastruey-Izquierdo, E. Mellado, M. Cuenca-Estrella, *J. Fungi* **2016**, 2, 21. <https://doi.org/10.3390/jof2030021>
- [42] P. Tiwari, P. Mishra, *J. Carcinog. Mutagen.* **2017**, 08, 4. <https://doi.org/10.4172/2157-2518.1000297>
- [43] S. B. Gopalakrishnan, T. Kalaiarasi, R. Subramanian, *J. Comput. Methods Phys.* **2014**, 2014, 1. <https://doi.org/10.1155/2014/623235>
- [44] D. Gadaleta, S. Manganelli, A. Manganaro, N. Porta, E. Benfenati, *Toxicology* **2016**, 370, 20. <https://doi.org/10.1016/j.tox.2016.09.008>
- [45] G. F. Smith, *Prog. Med. Chem.* **2011**, 50, 1.
- [46] R. Benigni, C. Bossa, *Chem. Rev.* **2011**, 111, 2507.
- [47] R. Benigni, C. Bossa, T. Netzeva, A. Rodomonte, I. Tsakovska, *Environ. Mol. Mutagen.* **2007**, 48, 754.
- [48] B. H. Hooberman, M. D. Brezzell, S. K. Das, Z. You, J. E. Sinsheimer, *Mutat. Res. Genet. Toxicol.* **1994**, 341, 57.
- [49] European Food Safety Authority, *EFSA J.* **2010**, 8, 1653.

## SUPPORTING INFORMATION

Additional supporting information may be found online in the Supporting Information section.

**How to cite this article:** Antypenko L, Sadykova Z, Shabelnyk K, et al. Synthesis and mode of action studies of novel {2-(3-R-1H-1,2,4-triazol-5-yl)phenyl}amines to combat pathogenic fungi. *Arch Pharm Chem Life Sci.* 2019;352: 1900092. <https://doi.org/10.1002/ardp.201900092>